

Supplementary Information

Electron-phonon interactions at the topological edge states in single bilayer Bi(111)

Enamul Haque^{1,2*}, Yuefeng Yin^{1,2*}, and Nikhil V. Medhekar^{1,2*}

¹ Department of Materials Science and Engineering, Monash University, Clayton, 3800 VIC, Australia

² ARC Centre of Excellence in Future Low Energy Electronics Technologies, Monash University, Clayton, 3800 VIC, Australia

* Corresponding author: enamul.haque@monash.edu, yuefeng.yin@monash.edu, nikhil.medhekar@monash.edu

S1. Computational Details

We considered a 2D crystal structure of single bilayer Bi(111) (SBB) in a supercell setting with a vacuum of 18 Å to avoid any spurious interactions between periodic images. For the implementation of density functional theory and density functional perturbation theory calculations, we used Quantum Espresso [1,2]. After extensive trials of the phonon calculations of SBB, we chose Vanderbilt scalar relativistic pseudopotential [3] for non-SOC calculations and fully relativistic pseudopotential from PSLibrary [4] for SOC calculations. Our trials suggest that these pseudopotentials can produce phonon dispersions of SBB with better accuracy than the norm-conserving and projector augmented wave pseudopotentials. The major advantage for the use of (Vanderbilt scalar relativistic or fully relativistic) ultrasoft pseudopotentials over the norm-conserving pseudopotential is that ultrasoft pseudopotential requires a much smaller cutoff energy to speed up the calculations. We selected the generalized gradient approximation [5] with Perdew-Burke-Ernzerhof functional for all calculations. Optimum cutoff energy and k -point (q -point) grid were determined by the convergence tests for the total energy. We found that 38 Ry (for scalar relativistic pseudopotential) – 45 Ry (for fully relativistic pseudopotential) cutoff energy for wave functions, 450–480 Ry cutoff energy for charge density, Gaussian smearing width 0.03-0.035 Ry, and $12 \times 12 \times 1 - 16 \times 16 \times 1$ k -point (661–881 q -point) are accurate enough to calculate phonon dispersions of SBB allowing the change of total energy less than 1 meV.

We fully relaxed (both lattice parameters and atomic positions) the structure of SBB using $16 \times 16 \times 1$ k -point and BFGS algorithm [6]. We performed these calculations with and without the SOC effect. We set a strict convergence criterion: self-consistency convergence threshold 10^{-7} Ry, energy convergence 10^{-07} Ry, and force convergence of 10^{-07}

Ry/Bohr. We performed phonon calculations using the same self-consistency convergence threshold, phonon convergence threshold 10^{-18} Ry, 881 q -point, and potential mixing parameter of 0.2. For electronic structure calculations, we considered a denser mesh, $24 \times 24 \times 1$ k -point. For electronic density of states and transport calculations, we used the optimized tetrahedron method. We kept the electron occupation fixed for dielectric and effective charge calculations.

Next, we built a 20-atoms zigzag and 24-atoms armchair nanoribbon supercells. We checked the feasibility of the phonon calculations including the SOC effect and found that electron-phonon calculations for armchair nanoribbons beyond 24-atoms are computationally infeasible. We then fully relaxed these structures using 45 Ry cutoff energy, $16 \times 1 \times 1$ ($1 \times 16 \times 1$) k -point, and self-consistency convergence of 10^{-10} Ry.

The average electron-phonon coupling matrix was obtained through the moving least square method implemented in EPAMLS (with 30 bins and Gaussian smoothing parameter 0.25) [7]. In the moving least square approach, the average e-ph matrix for each electronic energy pair ϵ_1 and ϵ_2 is obtained through the following equation [7]

$$g_v^2(\epsilon_1, \epsilon_2) = \frac{1}{W_1} \sum_{mnkq} w_{mnkq} |g_{mnv}^{SE}(k, q)|^2 \dots\dots(S1)$$

where $W_1 = \sum_{mnkq} w_{mnkq}$. Here $|g_{mnv}^{SE}(k, q)|^2$ is the weighted mean of momentum dependent e-ph matrix and w_{mnkq} is each sample weight, which includes the Gaussian scaling factor of the Gaussian function and the sample point degeneracy in the Brillouin zone. We calculated electrical conductivity and carrier lifetime using BoltzTraP code [8] by solving a semiclassical Boltzmann transport equation with energy eigenvalue (obtained from Quantum Espresso) and average e-ph matrix (obtained from EPAMLS code).

The e-ph coupling calculations were performed by using the interpolation technique [9] in Quantum Espresso. The e-ph coupling constant (λ) is defined by

$$\lambda = \sum_{qv} \lambda_{qv} = \frac{\gamma_{qv}}{\pi N(\epsilon_F) \omega_{qv}^2} \dots\dots(S2)$$

where the phonon linewidth γ_{qv} is expressed as [9]

$$\gamma_{qv} = 2\pi\omega_{qv} \sum_{mn} \sum_k |g_{k+q,k}^{qv,mn}|^2 \delta(\varepsilon_{k+q,m} - \varepsilon_F) \delta(\varepsilon_{k,n} - \varepsilon_F) \dots\dots\dots(S3)$$

Here $N(\varepsilon_F)$ is the density of states at the Fermi energy ε_F , ω_{qv} and $g_{k+q,k}^{qv,mn}$ describe the phonon energy and electron-phonon coupling for electron wavevector k and phonon wavevector q .

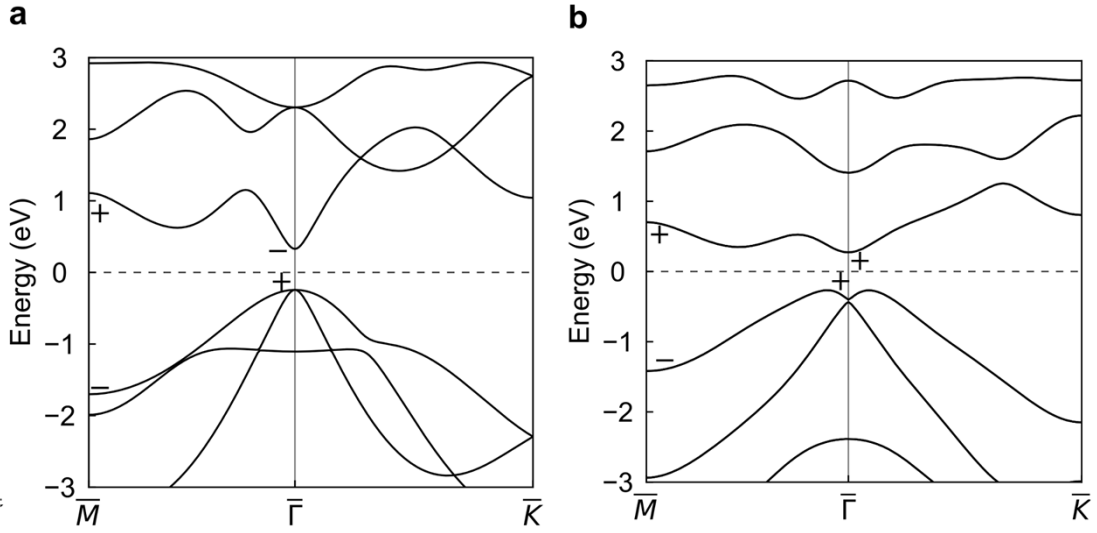


Fig. S1. Electronic band structure of single bilayer Bi(111) with (a) and without (b) SOC effect. The + and - symbols indicate the calculated parity at the high symmetry points.

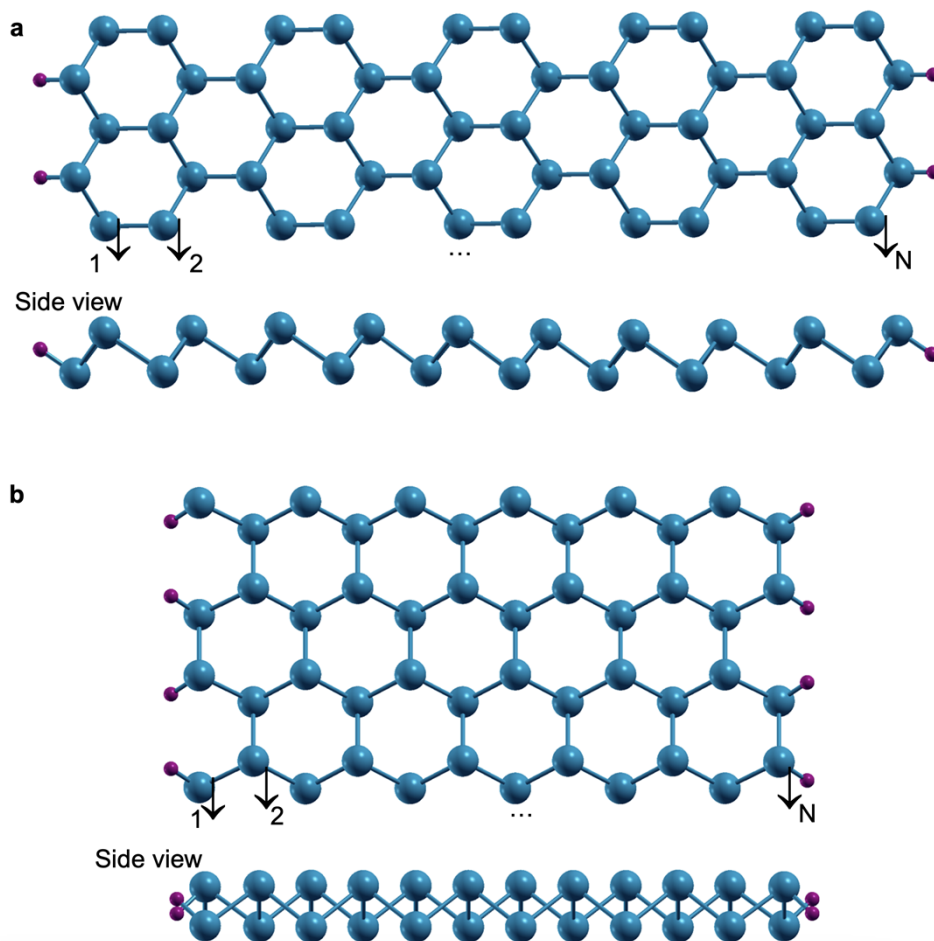


Fig. S2: (a) Extended top view of fully relaxed H-passivated zigzag nanoribbon and its side view. (b) Extended top view of fully relaxed H-passivated armchair nanoribbon and its side view. The numbers 1, 2, ...,N indicates the width of the ribbon. The native nanoribbons have the same structure excluding hydrogen and are not shown here.

Table S1. Fully relaxed lattice parameters (a, b), and macroscopic dielectric constant (ϵ), computed based on scalar relativistic (SR) (without SOC) and fully relativistic (with SOC) calculations.

Systems		a (Å)	b (Å)	ϵ
SBB	SR	4.307	4.307	7.09
	SOC	4.299	4.299	7.02
Zigzag edge	SR	4.222	-	--
	SOC	4.199	-	--
Passivated zigzag edge	SR	4.281	-	5.73
	SOC	4.263	-	--
Armchair edge	SR	-	7.437	3.98
	SOC	-	7.397	--
Passivated armchair edge	SR	-	7.423	3.83
	SOC	-	7.336	--

The dielectric constant is a pivotal parameter in explaining the electronic structure of insulators/semiconductors. Table S1 lists the calculated dielectric constant. The calculated value of the dielectric constant of SBB is almost the same as that reported for monolayer MoS₂ (7.36) [10]. The SOC has a negligible effect on the dielectric properties of SBB. Interestingly, the dielectric constant depends on the orientation of the edge, as its magnitude for armchair edge or passivated armchair edge is almost half that of zigzag edge or passivated zigzag edge. The dielectric constant along the vacuum direction is ~ 1 for all calculated cases, as expected.

References

- [1] P. Giannozzi *et al.*, Journal of Physics: Condensed Matter **21**, 395502 (2009).
- [2] P. Giannozzi *et al.*, The Journal of Chemical Physics **152**, 154105 (2020).
- [3] D. Vanderbilt, Physical Review B **41**, 7892 (1990).
- [4] A. Dal Corso, Computational Materials Science **95**, 337 (2014).
- [5] J. P. Perdew, K. Burke, and M. Ernzerhof, Physical Review Letters **77**, 3865 (1996).
- [6] R. Fletcher, *Practical methods of optimization* (John Wiley & Sons, 2013).
- [7] S. Bang, J. Kim, D. Wee, G. Samsonidze, and B. Kozinsky, Materials Today Physics **6**, 22 (2018).
- [8] G. K. Madsen and D. J. Singh, Computer Physics Communications **175**, 67 (2006).
- [9] M. Wierzbowska, S. de Gironcoli, and P. Giannozzi, 2005), ArXiv Preprint Cond-mat/0504077
- [10] A. Molina-Sanchez and L. Wirtz, Physical Review B **84**, 155413 (2011).